J Wood Sci (2014) 60:305–312
DOI 10.1007/s10086-014-1416-0

ORIGINAL ARTICLE

Modeling the effects of growth rate on the intra-tree variation in basic density in hinoki cypress (*Chamaecyparis obtusa*)

Junji Kimura · Takaaki Fujimoto

Received: 6 December 2013 / Accepted: 17 June 2014 / Published online: 25 July 2014

Abstract The purpose of this study is to evaluate the effect of growth rate on intra-tree variation in basic density of hinoki cypress (*Chamaecyparis obtusa*) quantitatively using the statistical modeling technique. Nineteen sample trees were harvested from 50-year-old hinoki stand which consists of two different growth rate plots. Disks were cut from sample trees at height positions of 2, 4 m, and then 4 m intervals until 16 m position. Radial strips were cut from the disks, and ring widths and basic density were measured at 5-ring intervals. The basic density decreased with age at any height positions. The linear mixed model was fitted to the age trend data having two nested grouping levels, i.e., tree and position within tree. Models having various mean and covariance structures were tested in devising an appropriate wood density model. The model, consisting of the mean structure with quadratic function of cambial age was able to describe the intra-tree variation in basic density. The model containing the random effects which consist of effect of the tree level and vertical stem position level explained the density variation adequately. The growth rate did not show the significant effect on the basic density variation within the stem.

Keywords Basic density · Growth rate · Intra-tree variation · Linear mixed-effect model · *Chamaecyparis obtusa*

Introduction

Hinoki cypress (*Chamaecyparis obtusa*) is one of the most important commercial species in Japan and its afforestation area accounts for 25 % of all plantation forest area in Japan [1]. Historically, hinoki has been used as building materials because it shows remarkable mechanical properties and durability [2]. For instance, it is well known that Horyuji, the world's oldest wooden architecture, was built more than 1,300 years ago and hinoki was mainly used as its construction member [3]. However, the wood resources have shifted from natural forests to plantation forests recently, and thus the wood properties of hinoki from plantation forests would be different from the past situation. The correct recognition of the wood properties in current hinoki resources should be necessary for the adequate forest management and utilization.

Numerous studies have reported the variation of wood properties in a number of species [4]. However, many of these reports are not quantitative examinations but qualitative examinations, except for the genetic variation which provides various genetic parameters. If the variation patterns of wood properties can be formulated quantitatively, one can interpolate the data or extrapolate the future situations based on the formulae.

There may be no discussed matter with regard to wood quality variation than relationship between growth rate and wood properties [4]. Especially, the effects of growth rate on wood density have been studied intensively. In hinoki cypress, Hirai reported that high growth rate would

Part of this report was presented at the 25th Meeting of the Chugoku-Shikoku Branch of the Japan Wood Research Society, Tottori, September 2013.

J. Kimura · T. Fujimoto (✉)
Faculty of Agriculture, Tottori University, Tottori 680-8553, Japan
e-mail: tafujimoto@muses.tottori-u.ac.jp

J. Kimura
e-mail: kmrjj.3tr@gmail.com

produce wood having low basic density [5]. Fujiwara et al. [6] examined the variation of basic density of hinoki which was obtained from nine test stands, and reported that there were no significant differences between thinned stands and un-thinned stands. Growth rate affects wood properties at different tree ages, and ignoring this effect could result in growth rate being incorrectly identified as the cause of differing wood properties [7, 8].

Sequences of yearly measurements of wood characteristics are considered as longitudinal (time series) data, and the analysis of longitudinal data is able to evaluate the age effect on variation of these characteristics. In this case, these data are repeated measures made of the same characteristic on the same observational unit (tree, disk, and ring), and such data generally present temporal autocorrelation, heteroscedasticity, and nonstationarity of the mean [9–11]. The mixed-effects analysis technique is frequently used for such grouped data including longitudinal data, repeated measures data, and multilevel data [12, 13]. Correlations among observations made on the same subject or experimental unit can be modeled using random effects, random regression coefficients, and through the specification of a covariance structure. Recent studies have developed models predicting variation in wood properties within a stem or cross section using the mixed-effects analysis for many species, such as pine and spruce [14–21].

Although the general variation pattern of basic density within stem is well known in hinoki, there is little information available about the effects of growth rate on the variation pattern of basic density. The objective of this study is to evaluate the effect of growth rate on variation pattern of basic density within stem. The linear mixed-effects model was used to explain the variation pattern of basic density quantitatively, and the effects of growth rate on its variation were also assessed on the basis of statistical manner.

Materials and methods

Sample materials were obtained from 50-year-old hinoki cypress stands in Tottori University Forest located in Maniwa, Okayama (35°16′ N, 133°36′ E; approximately 540 m elevation). The annual average precipitation and temperature from 2002 to 2012 in the research forest were 1989 mm and 11.6 °C, respectively. Hinoki cypress seedlings were planted in 1962 at an initial plant density of 3333 trees/ha. The test stand consisted of four 10-m square plots, which were two fast growth plots and two slow growth plots. They were adjacent to each other. The information of the test stand is summarized in Table 1. Although the detailed archive of the stand is unclear, the fast growth plots had been thinned several times. On the other hand, the slow growth plots have never been thinned previously. As a result, the stand density between them was quite different.

Table 1 Characteristics of the plots and sample trees in the test stand

	Plot A		Plot B	
	A1	A2	B1	B2
Stand density (tree/ha)	1000	1200	2100	2800
BA (m^2/ha)	50.9	52.5	63.2	42.0
DBH (cm)	22.8	20.9	19.9	13.6
Height (m)	17.6	17.5	17.2	11.5
BLC (m)	11.2	9.1	11.1	5.5

The data were obtained when the sample trees were harvested. DBH, Height, and BLC are the mean value of sample trees

BA basal area, *DBH* diameter at breast height, *BLC,* height to the base of live crown

From each plot, four or five, totally nineteen sample trees, were felled in 2012. Height and height to the base of live crown (BLC) of the sample trees were measured. The average height, DBH and BLC of sample trees were 15.9 m, 20.7 cm and 9.1 m, respectively. The height ranged from 10.2 to 18.6 m. DBH ranged from 11.9 to 30.9 cm. Analysis of variance confirmed the significant difference of the DBH among plots ($p = 0.006$; data not shown).

A 5-cm-thick, knot-free sample disks were cut from each sample tree at height positions of 2, 4 m, and then 4 m intervals until 16 m position. A 3-cm-thick radial strip was cut from each disk and ring width was measured from pith to outward in every five rings. Radial diameter of sample strips ranged from 1.4 to 12.1 cm. The measurements were carried out for two radial directions and ring width was expressed as the mean of both values. After that, the strips were cut into every 5 rings for basic density analysis. Water displace method was used to determine the basic density. The basic density was also determined as the mean of both radial directions. Radial and longitudinal variations of basic density for each plot are presented in Fig. 1.

Model development

The start model

The mixed model technique [12, 13] was used for modeling the effects of growth rate on the intra-tree variation in basic density. Figure 1 indicates that basic density can be represented by the quadratic function of cambial age, i.e., ring number from pith. On the start model, the fixed effects consisted of population mean and effects of plots determined by growth rate. The random effects consisted of

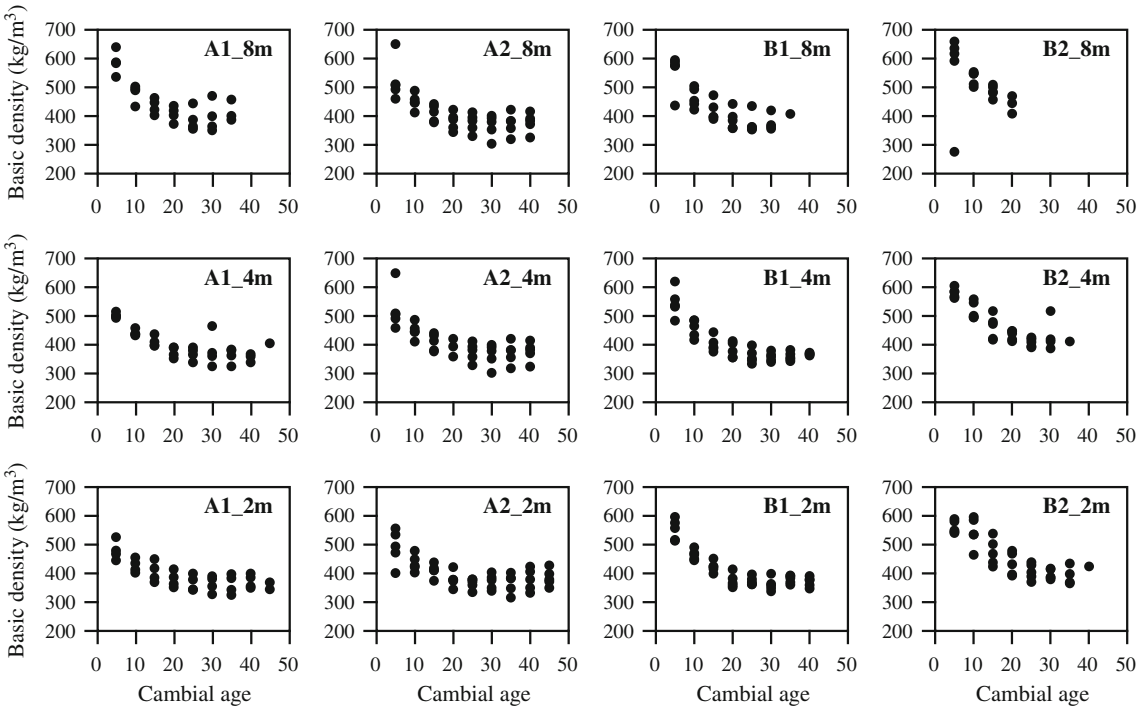

Fig. 1 Radial and longitudinal variations of basic density from different growth rate plots

effect of the tree level and vertical stem position level. The model expressed as

$$\begin{aligned} BD_{hijk} &= \left(\beta_0 + \beta_{0h} + b_{0i} + b_{0i,j}\right) + \left(\beta_1 + \beta_{1h} + b_{1i} + b_{1i,j}\right) AGE_k \\ &\quad + \left(\beta_2 + \beta_{2h} + b_{2i} + b_{2i,j}\right) AGE_k^2 + \varepsilon_{hijk}, \\ \boldsymbol{b}_i &= \begin{bmatrix} b_{0i} \\ b_{1i} \\ b_{2i} \end{bmatrix} \sim N(\mathbf{0},\ \boldsymbol{\Psi}_1), \quad \boldsymbol{b}_{i,j} = \begin{bmatrix} b_{0i,j} \\ b_{1i,j} \\ b_{2i,j} \end{bmatrix} \sim N(\mathbf{0},\ \boldsymbol{\Psi}_2), \\ \varepsilon_{hijk} &\sim N\left(0,\ \sigma^2\right), \end{aligned} \tag{1}$$

where BD_{hijk} was the basic density of the kth cambial age of the jth vertical stem position in the ith tree in the hth plot; β_0, β_1 and β_2 were the population mean of the basic density; β_{0h}, β_{1h} and β_{2h} were the fixed-effect parameters of hth plot; $\boldsymbol{b}_i$ was the tree-level random-effects vector; $\boldsymbol{b}_{i,j}$ was the position-level random-effects vector; ε_{hijk} was the within-group error. The $\boldsymbol{b}_i$ were assumed to be independent for different i, the $\boldsymbol{b}_{i,j}$ were assumed to be independent for different i, j and independent of the $\boldsymbol{b}_i$, and the ε_{hijk} were assumed to be independent for different i, j, k and independent of the random effects. The large number of parameters in Eq. (1) makes the optimization of the profiled log-restricted-likelihood quite difficult and unstable [12]. To make the optimization more stable during this model building phase, we simplify Eq. (1) by assuming $\boldsymbol{\Psi}_1$ and $\boldsymbol{\Psi}_2$ as diagonal matrices. The models in this article were fitted using the nlme package in R version 3.0.0 [22].

Selecting the fixed-effects structure

First, we evaluate whether the quadratic function of cambial age is adequate to describe the observed data and also test whether the growth rate has significant effect on the intra-tree variation on the basic density. The result of fitting indicated that both first- and second-order terms of age were highly significant ($p < 0.001$), and thus, the quadratic function of cambial age well describes the radial variation of basic density.

There were no clear effects in the terms of plot ($p = 0.087$), plot-AGE interaction ($p = 0.288$), and plot-AGE^2 interaction ($p = 0.079$). The results indicate that growth rate does not affect the variation pattern of basic density within the stem in hinoki cypress. Consequently, the fixed effect of the Eq. (1) could be simplified to the structure without plot effects.

Determining the variance–covariance structure of random effects

The age quadratic model without plot effects (model 1.1) was examined to determine the variance–covariance structure of random effects. The pair plot for the estimated random effects in the tree level is shown in Fig. 2. There was a weak positive correlation between the AGE and AGE^2 random effects, but no substantial correlation between either of these random effects and the intercept

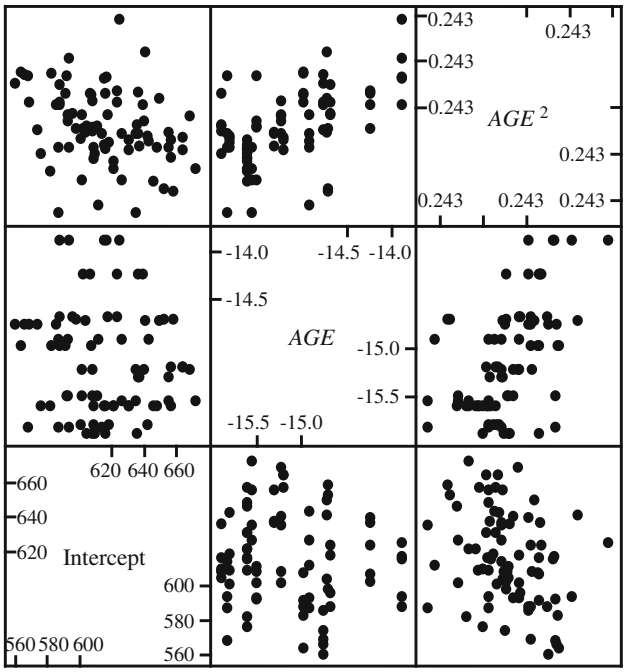

Fig. 2 Scatter plot of the estimated random effects in tree level from model 1.1

random effects. A blocked diagonal matrix can be used to represent such covariance structure [12], with the intercept random effect corresponding to one block and the *AGE* and AGE^2 random effects corresponding to another block. There was no remarkable correlation found among the random effects in the vertical stem position level.

Several models with different structures for the variance–covariance matrices of the estimated random effects were fitted and compared using the log-likelihood ratio test (LRT), the Akaike's information criterion (AIC), and the Schwarz's Bayesian information criterion (BIC). According to the fit statistics presented on Table 2, model 1.2 with the blocked diagonal matrix in the tree level was the best of the variance–covariance structure of random effects. Hence, the variance–covariance structure could be represented as

$$\mathrm{Var}\,(\boldsymbol{b}_i) = \boldsymbol{\Psi}_1 = \begin{bmatrix} \sigma_{00} & 0 & 0 \\ 0 & \sigma_{11} & \sigma_{12} \\ 0 & \sigma_{21} & \sigma_{22} \end{bmatrix}, \quad \mathrm{Var}\,(\boldsymbol{b}_{i,j}) = \boldsymbol{\Psi}_2 = \begin{bmatrix} \sigma_{00} & 0 & 0 \\ 0 & \sigma_{11} & 0 \\ 0 & 0 & \sigma_{22} \end{bmatrix} \tag{2}$$

Determining the structure of the within-group error

The within-group error, ε_{hijk}, were assumed to be independent for different i, j, k and independent of the random effects in model 1.2. The plots of residuals against the fitted values and other candidate variance covariates are useful for investigating within-group heteroscedasticity [12]. In this case, the cambial age is a natural candidate for the variance covariate. Figure 3 shows the plots of residuals versus *AGE*, indicating that the residuals decrease with *AGE*. Thus, we proceed by specifying the variance structure of the within-group error to account for heteroscedasticity. We use a conditional error variance [12, 23], where we assume

$$\mathrm{Var}\left(\varepsilon_{ijk} \mid \boldsymbol{b}_{i,j}, \boldsymbol{b}_{ij}\right) = \sigma^2 G^2\left(\mu_{ijk}, \upsilon_{ijk}, \delta\right), \tag{3}$$

where is $\mu_{ijk} = \mathrm{E}\,[y_{ijk} \mid \boldsymbol{b}_{i,j}, \boldsymbol{b}_{ij}]$, $\boldsymbol{\upsilon}_{ijk}$ is a vector of variance covariates, δ is a vector of variance parameters and $G(.)$ is the variance function. A number of variance function can be used in the nlme package, the following two variance structures were tested in this study. The first is the power model which is given as

$$\mathrm{Var}\left(\varepsilon_{ijk}\right) = \sigma^2 \left|\upsilon_{ijk}\right|^{2\delta}, \quad G\left(\upsilon_{ijk}, \delta\right) = \left|\upsilon_{ijk}\right|^{\delta} \tag{4}$$

The second is the exponential model which can be represented as

$$\mathrm{Var}\left(\varepsilon_{ijk}\right) = \sigma^2 \exp\left(2\delta\upsilon_{ijk}\right), \quad G\left(\upsilon_{ijk}, \delta\right) = \exp\left(\delta\upsilon_{ijk}\right) \tag{5}$$

The parameter δ is unrestricted, thus, the both variance structures can model a case where the variance increases or decreases with the variance covariate. There were significant increases in the log-restricted-likelihood, as evidenced

Table 2 Comparisons of the model performance with different variance–covariance structures for the random effects

Model	Var–Cov structure		No. of parameters	AIC	BIC	logLik	LRT	*p* value
	Tree	Position						
1.1	Diag	Diag	13	4808	4850	−2393.9		
1.2	Block-diag	Diag	11	4794	4840	−2386.1	15.7	0.00001
1.3	Diag	Block-diag	11	4810	4856	−2393.9	<0.001	0.9996
1.4	Block-diag	Block-diag	12	4796	4864	−2386.1	15.7	0.00004

Diag diagonal matrix structure, *Block-Diag* blocked diagonal matrix structure, *logLik* log-restricted-likelihood estimated by restricted maximum likelihood method, *AIC* Akaike's information criterion, *BIC* Schwarz's Bayesian information criterion *LRT* likelihood ratio test calculated with respect to model 1.1

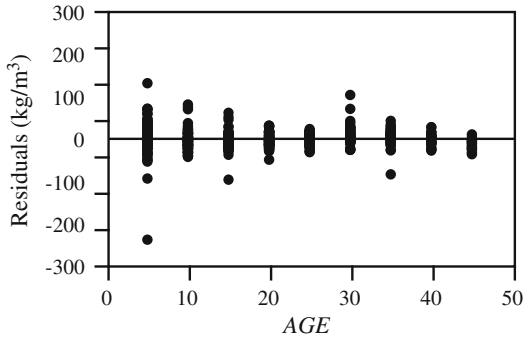

Fig. 3 Plot of residuals versus cambial age for the model 1.2 having homoscedastic within-group errors

by the large value of the LRT, indicating that addition of the variance function to the model significantly improves on model 1.2 (Table 3). Based on AIC and BIC, power function of age (model 1.2.1) will be used to represent variance structure of the within-group error.

Since the age trend of basic density could be considered as time series data, we need to pay attention to the temporal autocorrelation. Serial correlation structures are used to model dependence in time series data [24]. The empirical autocorrelation function provides a useful tool for investigating serial correlation in time series data. A plot of the estimated autocorrelation coefficients against lags for model 1.2.1 indicates that autocorrelations were significant even at cambial age lag 3 and 4 (data not shown). The following second-order moving average MA(2) was the best of the candidate correlation structures based on the statistics presented in Table 4.

$$\varepsilon_t = \sum_{j=1}^{2} \theta_j a_{t-j} + a_t, \tag{6}$$

where ε_t is the current within-subject error term, θ_j are the moving-average parameters ($j = 1, 2$) and a_t is a homoscedastic noise term centered at 0 ($\mathrm{E}[a_t] = 0$). The estimated normalized autocorrelation structure for model 1.2.1.4 residuals was

$$\begin{aligned}\hat{\rho} &= [\hat{\rho}(1),\ \hat{\rho}(2),\ \hat{\rho}(3),\ \hat{\rho}(4),\ \hat{\rho}(5),\ \hat{\rho}(6), \hat{\rho}(7), \hat{\rho}(8)]^{\mathrm{T}} \\ &= [-0.198,\ -0.087,\ -0.112,\ -0.194,\ -0.098, \\ &\quad -0.042,\ -0.097]^{\mathrm{T}},\end{aligned} \tag{7}$$

where $\hat{\rho}(l)$ is the empirical autocorrelation calculated at lag l and the estimated parameters for the MA(2) model were $\theta_1 = 0.348$, and $\theta_2 = 0.256$.

We selected the MA(2) model that is more adequate to represent the autocorrelation at small lags even though the second-order autoregressive model AR(2) model and the MA(2) model indicated almost the same AIC, BIC and log-restricted-likelihood. This is because the empirical autocorrelation at larger lags tends to be less reliable due to the estimation by fewer residuals pairs [12]. In our data, there were differences of the ring number from pith among the disks. For example, a total ring number of a disk was 42 while that of another was only 37, such disproportion of the

Table 3 Comparisons of the model performance with different within-group error variance structures

Model	Variance function	No. of parameters	AIC	BIC	LogLik	LRT	*p* value
1.2	No structure	11	4794	4840	−2386.1		
1.2.1	Power	12	4646	4697	−2311.2	150.0	<0.0001
1.2.2	Exponential	12	4682	4732	−2329.2	113.8	<0.0001

Likelihood ratio test calculated with respect to model 1.2. Abbreviations are same in Table 2

Table 4 Comparisons of the model performance with different within-groups correlation structures

Model	Correlation structure	No. of parameters	AIC	BIC	LogLik	Test	LRT	*p* value
1.2.1	Independent	12	4646	4697	−2311.2			
1.2.1.1	AR (1)	13	4623	4678	−2298.7	1.2.1 versus 1.2.1.1	25.0	<0.0001
1.2.1.2	AR (2)	14	4621	4680	−2296.6	1.2.1.1 versus 1.2.1.2	4.1	0.0419
1.2.1.3	MA (1)	13	4632	4686	−2303.0	1.2.1.2 versus 1.2.1.3	12.7	0.0004
1.2.1.4	MA (2)	14	4621	4680	−2296.7	1.2.1.3 versus 1.2.1.4	12.6	0.0004
1.2.1.5	ARMA (1,1)	14	4622	4681	−2297.2			
1.2.1.6	ARMA (1,2)	15	4622	4685	−2296.0	1.2.1.5 versus 1.2.1.6	1.7	0.1872
1.2.1.7	ARMA (2,1)	15	4623	4685	−2296.4			

AR autoregressive model, *MA* moving average correlation model, *ARMA* mixed autoregressive-moving average model, Other abbreviations are same in Table 2

Table 5 The estimated fixed effects parameters of basic density with the quadratic function of cambial age

Parameters	Estimate	Std. error	p value
β_0	598.8215	7.9846	<0.0001
β_1	−13.1779	0.7004	<0.0001
β_2	0.1978	0.0132	<0.0001

data also might be possibly the cause of the autocorrelation at larger lags.

Final model

We have tested the models having various mean and covariance structures, and have finally obtained the following model to describe the intra-tree variation in basic density.

$$
\begin{aligned}
BD_{ijk} &= \left(\beta_0 + b_{0i} + b_{0i,j}\right) + \left(\beta_1 + b_{1i} + b_{1i,j}\right) AGE_k \\
&\quad + \left(\beta_2 + b_{2i} + b_{2i,j}\right) AGE_k^2 + \varepsilon_{ijk}, \\
\boldsymbol{b}_i &\sim N\left(\mathbf{0}, \begin{pmatrix} \sigma_{00} & 0 & 0 \\ 0 & \sigma_{11} & \sigma_{12} \\ 0 & \sigma_{21} & \sigma_{22} \end{pmatrix}\right), \ \boldsymbol{b}_{i,j} \sim N\left(\mathbf{0}, \begin{pmatrix} \sigma_{00} & 0 & 0 \\ 0 & \sigma_{11} & 0 \\ 0 & 0 & \sigma_{22} \end{pmatrix}\right), \\
\varepsilon_{ijk} &\sim N\left(0, \ \sigma^2 G_{ijk}^{1/2}\left(v_{ijk}, \ \delta\right) H_{ijk}(\varphi, \ \theta) \ G_{ijk}^{1/2}\left(v_{ijk}, \ \delta\right)\right), \\
G_{ijk}\left(v_{ijk}, \ \delta\right) &= |AGE|^{\delta}, \quad H_{ijk}(\varphi, \ \theta) = \mathrm{ARMA}(0, \ 2),
\end{aligned}
\tag{8}
$$

where H_{ijk} $(\phi, \ \theta)$ is the serial correlation function and ARMA is mixed autoregressive-moving average model. The remaining elements of the model have been described previously. Parameter estimates, corresponding standard errors and p values for fixed effects of model 1.2.1.4 [Eq. (8)] are given in Table 5.

A final assessment of the adequacy of model 1.2.1.4 [eq. (8)] is given by the plot of the augmented prediction [12, 19] for a chosen tree (Fig. 4). Observed values of basic density, prediction by estimated fixed-effects parameters of model 1.2.1.4, which random effects were excluded, and that of containing random effects. The predictions containing the random effects follow the observed values closely, indicating that the final model explains the density variation data well.

Discussion

This study applied the linear mixed model to evaluate the effects of growth rate on the intra-tree variation in the basic density. The basic density decreased from pith to outward and the unique pattern was found in any height position (Fig. 1). The results were consistent with the previous reports in hinoki cypress [25, 26]. From Fig. 4, the final model with the quadratic function of cambial age [Eq. (8)]

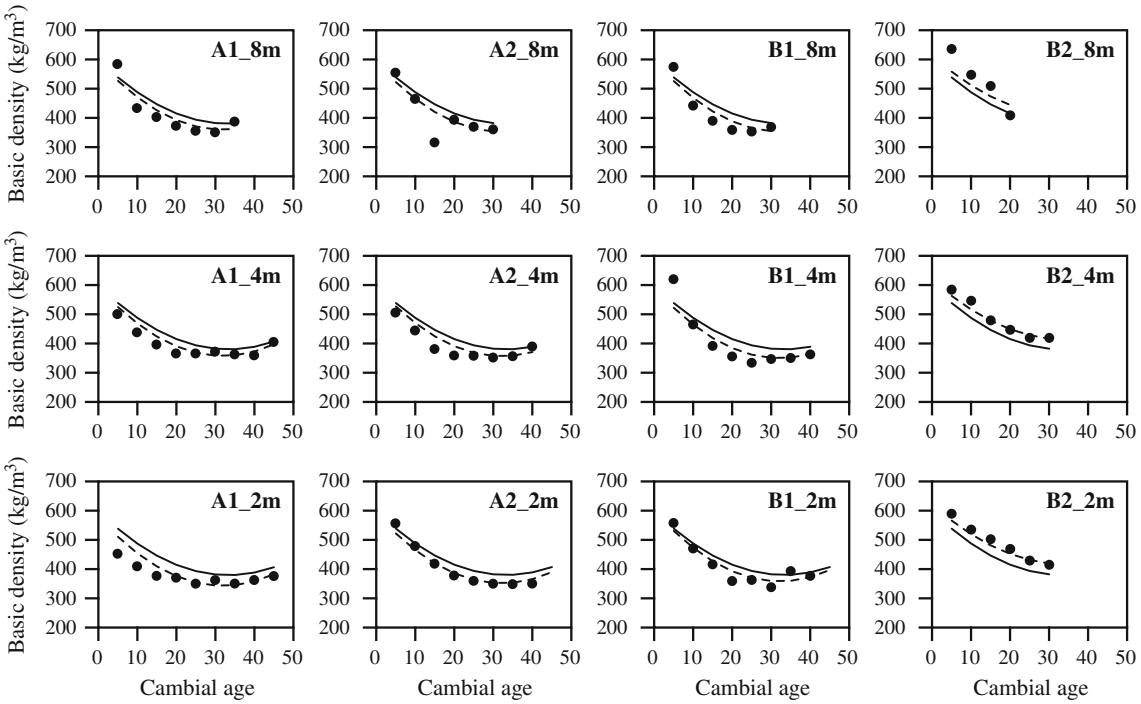

Fig. 4 Population prediction (setting all random effects to 0), subjects specified prediction (containing random effects) from the final model 1.2.1.4 and observed values of basic density versus cambial age. The solid lines, the dots line and filled circles indicate the population prediction, subjects specified prediction and observed values, respectively

explained the variation of basic density successfully. The density variation pattern found in hinoki is different from those of general coniferous tree, such as pine and larch, where the wood density increases with age [4, 7]. Decrease of wood density with age can be also found in sugi (*Cryptomeria japonica*) [26, 27].

There were no significant effects in the terms of plot, plot-*AGE* interaction, and plot-AGE^2 interaction. The results indicate that growth rate does not affect the variation pattern of basic density within the stem in hinoki cypress. There were few studies about the effects of growth rate on the variation pattern of basic density in hinoki cypress in spite of its importance for forest management and utilization. Fujiwara et al. [6] reported the similar results, but Hirai's report [5] is inconsistent with our result. Growth rate affects wood density at different tree ages, and the inconsistency of these results would be due to the ignorance of age effects [4, 8]. The modeling approach employed in this study can assess the effects of growth rate on the variation of wood density quantitatively considering the age effects. The effect of growth rate on wood density varies greatly among species [4], and it can be confirmed that hinoki shows the similar tendency as the hard pines, Douglas-fir, and larch species.

The defining characteristics of mixed-effects models are that they are applied to data where the observations are grouped according to one or more levels of experimental units and that they incorporate both fixed-effects terms and random-effects term [12]. Moreover, they present an inherent flexibility that allows for development of a unique variance–covariance structure alleviating the problems of nonconstant variance and autocorrelation among the repeated measurements. The final model has two levels of mixed effects with random effects at the tree and vertical position levels. The random-effects estimates were found to be larger at the tree level than the vertical position level (data not shown). This means that the basic density values at each height position are relatively consistent, but the variation among trees is more noticeable, due to the unique patterns of basic density corresponding to height level.

In this study, the variation of wood density within stem was modeled using the linear mixed-effects model. The methodology presented in this paper can easily extend for other wood properties [16, 18–20, 28]. In this case, it should be noted that the age trend of each traits is quite different. For instance, tensile strength in hinoki increases from pith to outward [29], and thus, the fitting model function should be different from that of wood density. We used the polynomial model that is linear in the parameters. By increasing the order of a polynomial model, one can get increasingly accurate approximations to the true regression function within the observed range of the data [12]. These empirical models are based only on the observed relationship between the response and the covariates and do not include any theoretical considerations about the underlying mechanism producing the data. As the next step, it would be useful to apply the nonlinear model that is based on a model for the mechanism producing the response, and that also provides more reliable predictions for the response variable outside the observed range of the data [16, 19, 20].

Acknowledgments The authors are grateful to Dr. Keisuke Kawakami of Tottori Prefectural Agriculture and Forest Research Institute for preparing the test specimens. We also deeply acknowledge Mr. Shogo Fukutomi and Ms. Asami Yoneda of Tottori University Forest for harvesting the sample trees.

References

1. Forestry Agency (2013) Annual report on trends in forests and forestry, fiscal year 2012 (summary). http://www.rinya.maff.go.jp/j/kikaku/hakusyo/24hakusyo/pdf/h24summary.pdf. Accessed 3 Oct 2013
2. Forests and Forestry Products Research Institute (1982) Wood technology and wood utilization division: properties of important Japanese woods table of the properties of woods (Research note) (in Japanese with English summary). Bull For For Res Inst 319:85–126
3. Nishioka T, Kohara J (2007) Horyuji wo sasaeta ki (in Japanese). NHK Publishing Co Ltd, Tokyo, pp 37–51
4. Zobel BJ, Buijtenen JP (1989) Wood variation. Its cause and control. Springer-Verlag, Berlin, pp 157–188
5. Hirai S (1958) Studies on weight growth of forest trees VI: *Chamaecyparis obtusa* in the Tokyo University Forest in Chiba (in Japanese with English summary). Bull Tokyo Univ For 54:199–217
6. Fujiwara T, Yamashita K, Hirakawa Y (2004) Mean basic density and density variation within individual trees in major plantation species (in Japanese with English summary). Bull FFPRI 3:341–348
7. Zobel BJ, Sprague JR (1998) Juvenile wood in forest trees. Springer-Verlag, Berlin, pp 113–140
8. Bendtsen BA (1978) Properties of wood from improved and intensively managed trees. For Prod J 28:61–72
9. Diggle P (1990) Time series: a biostatistical introduction. Oxford University Press, Oxford, pp 134–164
10. Tasissa G, Burkhart HE (1998) Modeling thinning effects on ring specific gravity of loblolly pine (*Pinus taeda* L.). For Sci 44:212–223
11. Herman M, Dutilleul P, Avella-Shaw T (1998) Growth rate effects on temporal trajectories of ring width, wood density, and mean tracheid length in Norway spruce [*Picea abies* (L.) Karst.]. Wood Fiber Sci 30:6–17
12. Pinheiro JC, Bates DM (2000) Mixed-effects models in S and S-PLUS. Springer-Verlag, New York, pp 1–270
13. Verbeke G, Molenberghs G (1997) Linear mixed models in practice—a SAS-oriented approach. Springer, Berlin Heidelberg New York, pp 63–153
14. Wilhelmsson L, Arlinger J, Spångberg K, Lundqvist SO, Grahn T, Hedenberg Ö, Olsson L (2002) Models for predicting wood properties in stems of *Picea abies* and *Pinus sylvestris* in Sweden. Scand J For Res 17:330–350

15. Guilley E, Hervé JC, Nepveu G (2004) The influence of site quality, silviculture and region on wood density mixed model in *Quercus petraea* Liebl. For Ecol Manag 189:111–121
16. Jordan L, Daniels RF, Clark A III, He R (2005) Multilevel nonlinear mixed-effects models for the modeling of earlywood and latewood microfibril angle. For Sci 51:357–371
17. Molteberg D, Høibø O (2007) Modelling of wood density and fibre dimensions in mature Norway spruce. Can J For Res 37:1373–1389
18. Mäkinen H, Jaakkola T, Piispanen R, Saranpää P (2007) Predicting wood and tracheid properties of Norway spruce. For Ecol Manag 241:175–188
19. Mora CR, Allen HL, Daniels RF, Clark A III (2007) Modeling corewood–outerwood transition in loblolly pine using wood specific gravity. Can J For Res 37:999–1011
20. Schneider R, Zhang SY, Swift DE, Bégin J, Lussier JM (2008) Predicting selected wood properties of jack pine following commercial thinning. Can J For Res 38:2030–2043
21. Repola J (2006) Models for vertical wood density of Scots pine, Norway spruce and birch stems, and their application to determine average wood density. Silv Fenn 40:673–685
22. Pinheiro J, Bates D, DebRoy S, Sarkar D (2013) nlme: Linear and nonlinear mixed effects models. R package, version 3.1, p 111
23. Davidian M, Giltinan DM (1995) Nonlinear models for repeated measurement data. Chapman and Hall, London, pp 97–124
24. Box GEP, Jenkins GM, Reinsel GC (1994) Time series analysis: forecasting and control, 4th edn. John Wiley & Sons Inc, Hoboken, pp 47–91
25. Koga S, Oda K, Tutsumi J, Koga H (1992) Wood property variations within a stand of hinoki (*Chamaecyparis obtusa*) and karamatsu (*Larix leptolepis*) (in Japanese with English summary). Bull Kyushu Univ For 66:55–68
26. Ishizuka F, Yokota S, Iizuka K, Saito K, Yoshizawa N (2004) Wood quality of conifers planted in Utsunomiya University Forests (in Japanese with English summary). Bull Utsunomiya Univ For 40:69–76
27. Yahata H, Miyajima H, Sairinji T, Huruie H, Kodoma T, Yuruki T, Yamamoto H, Kubota S, Watanabe K, Nogami K, Kuroki H (1987) Wood quality variations of native cultivars and the clones of plus trees in the experimental areas of cultivars of *Cryptomeria japonica* in Kyushu (in Japanese with English summary). Bull Kyushu Univ For 57:149–173
28. Alteyrac J, Cloutier A, Ung CH, Zhang SY (2006) Mechanical properties in relation to selected wood characteristics of black spruce. Wood Fiber Sci 38:229–237
29. Suzuki M (1968) The relationship between elasticity and strength properties and cell structure of coniferous wood (in Japanese with English summary). Bull For For Res Inst 212:89–149